

# Effect of Hydrothermal Temperature on the Morphology and Structure of Synthesized MoS<sub>2</sub> Nanostructures

*Le Thi Hong, Vy Anh Vuong, Nguyen Tat Thang, Nguyen Xuan Thai,  
Nguyen Van Toan, Dang Thi Thanh Le, Chu Manh Hung\**

*Hanoi University of Science and Technology – No. 1, Dai Co Viet Str., Hai Ba Trung, Ha Noi, Viet Nam*

*Received: August 10, 2018; Accepted: November 28, 2019*

## Abstract

The MoS<sub>2</sub> nanostructures with different morphologies were synthesized by a facile hydrothermal method using precursors of ammonium molybdate ((NH<sub>4</sub>)<sub>6</sub>Mo<sub>7</sub>O<sub>24</sub>·4H<sub>2</sub>O), thiourea (CH<sub>4</sub>N<sub>2</sub>S) and hydroxylammonium chloride (NH<sub>2</sub>OH.HCl). As-prepared MoS<sub>2</sub> samples with different growth temperatures of 160, 180, and 200 °C were characterized by Raman spectroscopy, field emission scanning electron microscopy (FESEM) and x-ray powder diffraction (XRD). Raman data of all samples showed the two active modes at about 380 cm<sup>-1</sup> and 406 cm<sup>-1</sup>, which were corresponding to in-plane vibration of Mo and S atoms as well as to out-of-plane vibration of S atoms of MoS<sub>2</sub> nanostructures. XRD results also revealed characteristic diffraction peaks of the MoS<sub>2</sub> for all samples grown at different temperatures. However, the XRD pattern of the MoS<sub>2</sub> grown at 200 °C exhibited a more pronounced peak at approximately 12.1°, corresponding to the diffracted peak of (002) lattice plane of MoS<sub>2</sub>. It implied that the MoS<sub>2</sub> nanostructures synthesized at 200 °C showed a better crystallinity compared to the rest. The findings indicated that reaction temperature has significant effects on the morphology and crystal structure of the as-prepared products. It was found that the optimal growth temperature was 200 °C. Under this condition, the nanostructures are about more than 100 nm in length and 10 nm in thickness.

Keywords: Hydrothermal, MoS<sub>2</sub>, growth temperature, Raman, XRD

## 1. Introduction

In the group of transition metal dichalcogenides (TMDs), molybdenum disulfide (MoS<sub>2</sub>) attracts much more attention due to their unique electrical, optical, mechanical properties compared to other materials owing to its tunable band gap energy (1.1-1.9) eV, high strength and high mobility [1–3]. Moreover, MoS<sub>2</sub> is also an environmentally friendly material. Thus, this material has excellent applicability in a variety of fields such as field effect transistors, catalysts, electrochemical and/or optoelectronic, energy storage devices, Li-ion batteries, and gas sensors [4–6]. Several types of MoS<sub>2</sub> nanostructures with different morphologies such as nanosheets, nanospheres, and nanoflowers, thin film have been synthesized by various methods such as hydrothermal method [7], mechanical or chemical exfoliation [8], chemical vapor deposition [9] and atomic layer deposition [10]. Among the various growth methods, the hydrothermal synthesis route has been considered to be one of the most promising synthesis routes, due to its low cost, high efficiency, and good crystallization of the product. To control the crystallinity and morphology,

synthesis temperature plays an important role in the hydrothermal synthesis of MoS<sub>2</sub> nanostructures. Recently, Wang *et al.* [11] has synthesized amorphous MoS<sub>2</sub> and discussed the effect on preparation temperature on crystallinity. Li *et al.* [12] prepared MoS<sub>2</sub> nanostructure with different morphologies when hydrothermal temperatures increased from 200 °C to 300 °C. The morphology of MoS<sub>2</sub> also changed from the coral-like aggregated particles to flower-like spheres wrapped nanosheet structure with temperature by Luo *et al.* [13].

Although several works have been reported on investigation of the effect of hydrothermal growth conditions of MoS<sub>2</sub>, there is lack of systematic study on the effect of low hydrothermal temperature below 200 °C to the formation of MoS<sub>2</sub>. In our previous work, we have moved a first step for hydrothermal synthesis of MoS<sub>2</sub> nanostructures [14]. In the present work, we study the effect of hydrothermal synthesis temperature on morphological and structural properties of MoS<sub>2</sub> nanostructures. The synthesized MoS<sub>2</sub> nanostructures

\*Corresponding author: Tel: (+84) 988138085

Email: hung.chumanh@hust.edu.vn

mhchu@itims.edu.vn

were characterized through SEM, XRD, and Raman spectroscopic measurements.

## 2. Experimental

MoS<sub>2</sub> nanostructures were synthesized through a simple hydrothermal method. In a typical synthesis, ammonium molybdate (0.617 g), thiourea (0.76 g) and hydroxylammonium chloride (0.69 g) were dissolved in 80 ml deionized water using a magnetic stirrer to form a homogeneous solution. Then, the obtained solution was poured into a 100 ml Teflon-line autoclave and sealed tightly, heated at 160 °C for 24h. After cooling to room temperature, the precipitated products were collected and washed several times using distilled water and ethanol solution by centrifugation at 4000 rpm and finally dried at 60 °C for 24 h. Other samples were also prepared in the same way with different preparation temperatures at 180 °C and 200 °C. Samples were marked as MoS<sub>2</sub>-160, MoS<sub>2</sub>-180 and MoS<sub>2</sub>-200 corresponding to the growth temperatures of 160 °C, 180 °C, and 200 °C, respectively. Fig. 1 shows the hydrothermal synthesis process of the MoS<sub>2</sub> nanostructures.

The morphologies of the synthesized materials were then examined by FESEM (JEOL JSM-7600F).

The crystal structures and vibrational modes of the MoS<sub>2</sub> nanostructures were characterized by XRD (Advance D8, Bruker) and Raman spectroscopy (Renishaw, InVia), respectively.

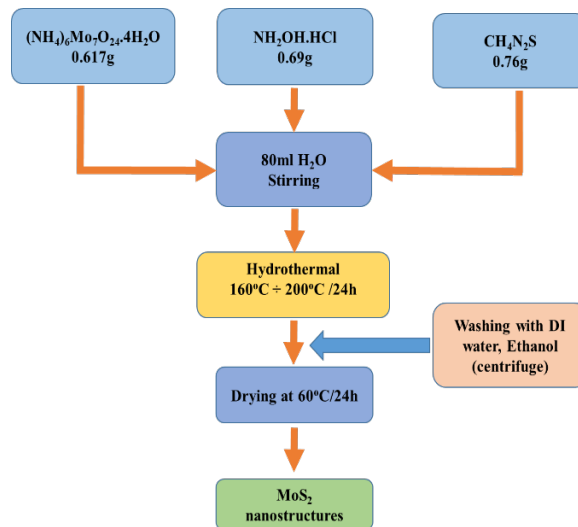


**Fig. 1.** Schematic diagram of the hydrothermal processes for the synthesis of the nanosheet MoS<sub>2</sub> nanostructures.

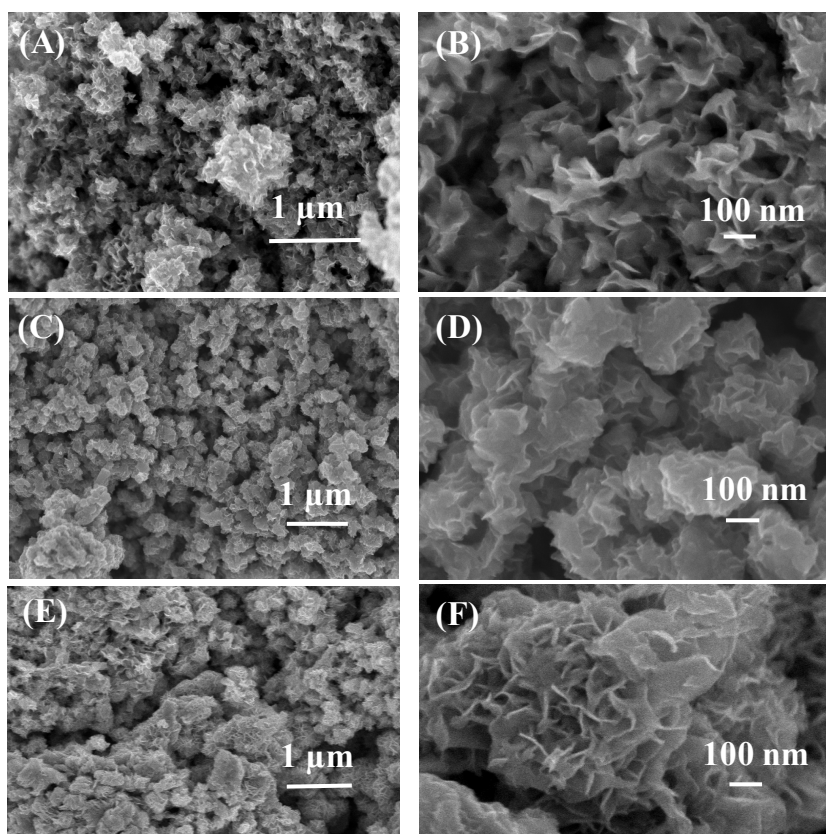


**Fig. 2.** SEM images of the nanosheet MoS<sub>2</sub> nanostructures fabricated with different preparation temperatures: (A and B) 160 °C; (C and D) 180 °C; (E and F) 200 °C.

### 3. Results and discussion

The morphologies of the MoS<sub>2</sub> nanostructures grown with different temperatures were characterized by SEM. The SEM images are shown in Fig. 2A-F. The results showed that the higher the hydrothermal temperature, the greater the number of nanosheet MoS<sub>2</sub> produced. The nanosheet-like MoS<sub>2</sub> nanostructures fabricated at 160 °C have been formed quite well. However, the size of the sheets is still small, and the length of the sheets is short (Fig. 2A-B). When the synthesis temperature was increased to 180 °C, the density of nanosheet became thicker but the sheets are still short with low stacking height (Fig. 2C-D). The SEM images of the MoS<sub>2</sub> nanostructures fabricated at 200 °C are shown in Fig. 2E-F. The nanosheets are about more 100 nm in length and 10 nm in thickness. Thus, the morphology of MoS<sub>2</sub> nanomaterials significantly changed because of the synthesis temperature conditions, it can be seen that when the hydrothermal temperature increases, the pressure in the closed vessel also increases, resulting in much more and faster MoS<sub>2</sub> products in a time unit due to the rate of reaction raising. At growth temperature of 200 °C, it seems that the MoS<sub>2</sub> nanosheets is thinner than that using other synthesis temperatures. In addition, the MoS<sub>2</sub> nanosheets were stacked together to form large MoS<sub>2</sub> nanostructure bunches in case of 200 °C growth temperature. For two lower synthesis temperatures of 160 °C and 180 °C, the nanostructure bunches generated from nanosheets are smaller and dispersed on the substrates.

Raman spectroscopy was employed to confirm the atom vibrational modes of MoS<sub>2</sub> nanostructures synthesized with different growth temperature of 160, 180, and 200 °C and growth time of 24h. The spectra of three structures, as shown in Fig. 3, exhibit two prominent Raman modes located at approximately 380 cm<sup>-1</sup> and 406 cm<sup>-1</sup> corresponding to the  $E_{2g}^1$  and  $A_{1g}$  vibrational modes of hexagonal MoS<sub>2</sub>, respectively. It is known that  $E_{2g}^1$  mode corresponds to the in-plane vibration of Mo and S atoms and  $A_{1g}$  mode corresponds to the out-of-plane vibration of S atoms of hexagonal MoS<sub>2</sub> [15]. It is obviously that the intensity of the  $A_{1g}$  peak is higher than that of the  $E_{2g}^1$ . This result is in agreement with other previous reports [3,16]. This can be due to the final state of direct electronic transition at K point related to  $d_{z^2}$  orbitals of Mo atoms, which are aligned along the identical oscillation direction of the  $A_{1g}$  mode [3,16,17]. This results in the enhancement of electron-phonon coupling along the out of plane direction ( $A_{1g}$ ). In addition to these two peaks, a mode around 455 cm<sup>-1</sup> arises from a second-order process involving the longitudinal acoustic phonons at M point ( $2LA(M)$ ) [3].

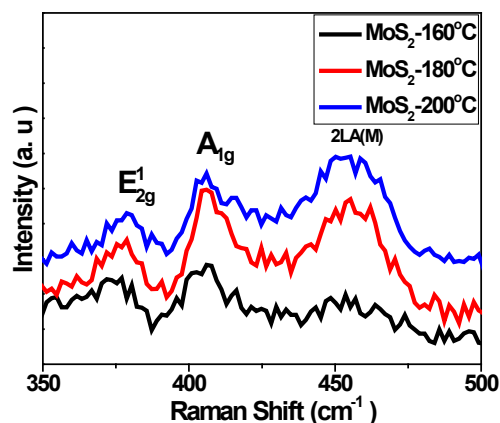


Fig. 3. Raman spectra of the MoS<sub>2</sub> nanostructures grown at 160, 180, and 200 °C.

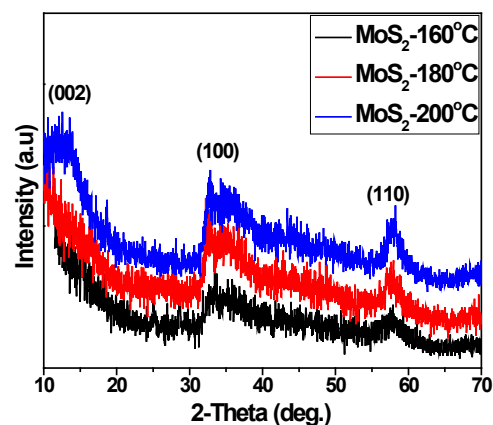


Fig. 4. XRD patterns of the synthesized MoS<sub>2</sub> nanostructures at various growth temperatures of 160, 180, and 200 °C.

Raman results indicated that featured vibration modes of the MoS<sub>2</sub> nanostructures were obtained for all three samples grown at 160, 180, and 200 °C. It is unobvious to point out the difference between these spectra. To study in more detail about the effect of growth temperature to the formation of the MoS<sub>2</sub> nanostructure and to get further inside into the crystallinity degree of the MoS<sub>2</sub> under different growth temperatures, Fig. 4 shows XRD patterns of MoS<sub>2</sub> nanostructures grown at different temperatures of 160 °C (black color), 180 °C (red color), and 200 °C (blue color). We can see that all three XRD patterns present clearly the diffraction peaks located at about 34.16° and 57.81°, which correspond to the (100) and (110) crystal planes of the MoS<sub>2</sub> [18]. However, with the increased temperature, the intensity of diffraction peaks becomes sharper, indicating the improvement of crystallinity with the raise of growth temperature. Especially, only XRD pattern of the MoS<sub>2</sub> nanostructures grown at 200 °C shows a peak centered at 12.1° corresponding to (002) crystal plane of the MoS<sub>2</sub> (JCPDS 37-1492). This result clearly indicates an improvement of the crystallinity degree of the MoS<sub>2</sub>

nanostructures grown at 200 °C compared to the ones grown at lower temperatures of 160 °C and 180 °C. The properties of the MoS<sub>2</sub> grown at 200 °C in this work can be comparable the MoS<sub>2</sub> formed with higher temperature of 260 °C from published work [12].

#### 4. Conclusion

In summary, the MoS<sub>2</sub> nanostructures were synthesized by a facile hydrothermal method. The morphology, vibrational modes, and crystal structures were investigated through SEM, Raman spectroscopic, and XRD measurements. The morphologies of the synthesized nanostructures were easily controlled by varying different preparation temperatures. The optimal growth temperature was found to be at 200 °C, in which the MoS<sub>2</sub> nanostructures formed under large bunches of thin MoS<sub>2</sub> sheets with high crystallinity degree. In order to obtain full story of the effect of growth conditions to the formation of MoS<sub>2</sub> nanostructures, the investigation of the effect of different growth times is necessary and will be presented in coming works.

#### Acknowledgments

This research was financially supported by Ministry of Education and Training under project No. B2018-BKA-08-CTrVL.

#### References

- [1] H. Dong, S. Tang, Y. Hao, H. Yu, W. Dai, G. Zhao, Y. Cao, H. Lu, X. Zhang, H. Ju; Fluorescent MoS<sub>2</sub> Quantum Dots: Ultrasonic Preparation, Up-Conversion and Down-Conversion Bioimaging, and Photodynamic Therapy; *ACS Appl. Mater. Interfaces*. 8 (2016) 3107–3114. doi:10.1021/acsami.5b10459.
- [2] S. Li, W. Zang, X. Liu, S.J. Pennycook, Z. Kou, C. Yang, C. Guan, J. Wang; Heterojunction engineering of MoSe<sub>2</sub>/MoS<sub>2</sub> with electronic modulation towards synergetic hydrogen evolution reaction and supercapacitance performance; *Chem. Eng. J.* (2018). doi:10.1016/j.cej.2018.11.036.
- [3] H. Li, Q. Zhang, C.C.R. Yap, B.K. Tay, T.H.T. Edwin, A. Olivier, D. Baillargeat; From bulk to monolayer MoS<sub>2</sub>: Evolution of Raman scattering; *Adv. Funct. Mater.* 22 (2012) 1385–1390. doi:10.1002/adfm.201102111.
- [4] Z. Li, J. Ma, Y. Zhou, Z. Yin, Y. Tang, Y. Ma, D. Wang; Synthesis of sulfur-rich MoS<sub>2</sub> nanoflowers for enhanced hydrogen evolution reaction performance, *Electrochim. Acta*. 283 (2018) 306–312. doi:10.1016/j.electacta.2018.06.135.
- [5] H. Yan, P. Song, S. Zhang, J. Zhang, Z. Yang, Q. Wang; A low temperature gas sensor based on Au-loaded MoS<sub>2</sub> hierarchical nanostructures for detecting ammonia; *Ceram. Int.* 42 (2016) 9327–9331. doi:10.1016/j.ceramint.2016.02.160.
- [6] Y. Zhong, Q. Zhuang, C. Mao, Z. Xu, Z. Guo, G. Li; Vapor phase sulfurization synthesis of interlayer-expanded MoS<sub>2</sub>@C hollow nanospheres as a robust anode material for lithium-ion batteries; *J. Alloys Compd.* 745 (2018) 8–15. doi:10.1016/j.jallcom.2018.02.163.
- [7] W.A. Publishing, N. York, HANDBOOK OF HYDROTHERMAL TECHNOLOGY A Technology for Crystal Growth and Materials Processing, n.d.
- [8] G. Cunningham, M. Lotya, C.S. Cucinotta, S. Sanvito, S.D. Bergin, R. Menzel, M.S.P. Shaffer, J.N. Coleman; Solvent exfoliation of transition metal dichalcogenides: Dispersibility of exfoliated nanosheets varies only weakly between compounds; *ACS Nano*. 6 (2012) 3468–3480. doi:10.1021/nn300503e.
- [9] P. Shen; Large-area CVD Growth of Two-dimensional Transition Metal Dichalcogenides and Monolayer MoS<sub>2</sub> and WS<sub>2</sub> Metal – oxide – semiconductor Field-effect Transistors by Master of Science in Electrical Engineering, (2017) 1–55.
- [10] B. Cho, M.G. Hahm, M. Choi, J. Yoon, A.R. Kim, Y.J. Lee, S.G. Park, J.D. Kwon, C.S. Kim, M. Song, Y. Jeong, K.S. Nam, S. Lee, T.J. Yoo, C.G. Kang, B.H. Lee, H.C. Ko, P.M. Ajayan, D.H. Kim; Charge-transfer-based gas sensing using atomic-layer MoS<sub>2</sub>, *Sci. Rep.* 5 (2015) 8052. doi:10.1038/srep08052.
- [11] D. Wang, Z. Pan, Z. Wu, Z. Wang, Z. Liu; Hydrothermal synthesis of MoS<sub>2</sub> nanoflowers as highly efficient hydrogen evolution reaction catalysts; *J. Power Sources*. 264 (2014) 229–234. doi:10.1016/j.jpowsour.2014.04.066.
- [12] W.J. Li, E.W. Shi, J.M. Ko, Z.Z. Chen, H. Ogino, T. Fukuda; Hydrothermal synthesis of MoS<sub>2</sub> nanowires; *J. Cryst. Growth*. 250 (2003) 418–422. doi:10.1016/S0022-0248(02)02412-0.
- [13] L. Luo, M. Shi, S. Zhao, W. Tan, X. Lin, H. Wang, F. Jiang; Hydrothermal synthesis of MoS<sub>2</sub> with controllable morphologies and its adsorption properties for bisphenol A; *J. Saudi Chem. Soc.* (2019). doi:10.1016/j.jscs.2019.01.005.
- [14] L.T. Hong, D. Thi, T. Le, C.M. Hung; CODE : THS-P06 Synthesis and characterization of MoS<sub>2</sub> nanostructures; *Int. Work. Adv. Mater. Sci. Nanotechnol. (IWAMSN 2018)*. (2018) 421–425.
- [15] G. Plechinger, J. Mann, E. Preciado, D. Barroso, a. Nguyen, J. Eroms, C. Schüller, L. Bartels, T. Korn; A direct comparison of CVD-grown and exfoliated MoS<sub>2</sub> using optical spectroscopy; *Phys. Rev. Lett.* 064008 (2013) 1–7. doi:10.1088/0268-1242/29/6/064008.
- [16] R. Coehoorn, C. Haas, R.A. de Groot, Electronic structure of MoSe<sub>2</sub>, MoS<sub>2</sub>, and WSe<sub>2</sub>. II. The nature of the optical band gaps, *Phys. Rev. B*. 35 (1987) 6203–6206. doi:10.1103/PhysRevB.35.6203.
- [17] V. Anh Vuong, C. Manh Hung; Direct Synthesis of Multi-layer MoS<sub>2</sub> Nanodots by Chemical Vapor Deposition; *Commun. Phys.* 28 (2018) 379. doi:10.15625/0868-3166/28/4/12650.
- [18] Y. Tian, Y. He, Y. Zhu; Low temperature synthesis and characterization of molybdenum disulfide nanotubes and nanorods; *Mater. Chem. Phys.* 87 (2004) 87–90. doi:10.1016/j.matchemphys.2004.05.010.